Dispersion relations for the anomalous magnetic moment of the muon

Peter Stoffer

Physics Department, UC San Diego

in collaboration with M. Hoferichter

JHEP **1907**, 073 (2019),

with G. Colangelo and M. Hoferichter

JHEP **1902**, 006 (2019),

and with G. Colangelo, M. Hoferichter, and M. Procura

JHEP **04** (2017) 161, PRL **118** (2017) 232001,
JHEP **09** (2015) 074, JHEP **09** (2014) 091,
and work in progress

27th August 2019

Lattice QCD workshop, Santa Fe, NM

1. Hadronic contributions to the muon $g-2$
2. Hadronic vacuum polarisation
   - Dispersion relation for the pion vector form factor
   - Fit strategy
   - Fit results and contribution to the muon $g-2$
3. Hadronic light-by-light scattering
   - Tensor decomposition and Mandelstam representation
   - Pion pole
   - Pion box
   - $\pi\pi$-rescattering
4. Conclusions and outlook

Hadronic vacuum polarisation (HVP)

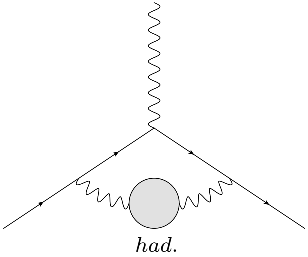

- problem: QCD is non-perturbative at low energies
- much progress using lattice QCD first-principle calculations
- best current evaluations based on dispersion relations and data (or combinations with lattice)

Hadronic vacuum polarisation (HVP)

Photon HVP function:

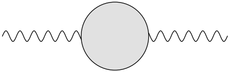 $= i(q^2 g_{\mu\nu} - q_\mu q_\nu)\Pi(q^2)$

Unitarity of the S-matrix implies the optical theorem:

$$\mathrm{Im}\Pi(s) = \frac{s}{e(s)^2}\sigma(e^+e^- \to \mathrm{hadrons})$$

Dispersion relation

Causality implies analyticity:

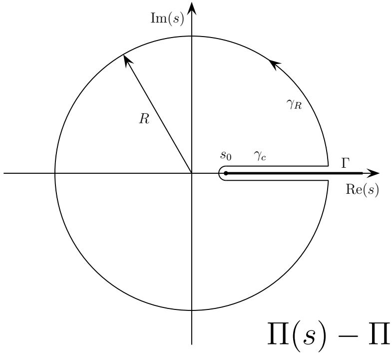

Cauchy integral formula:

$$\Pi(s) = \frac{1}{2\pi i} \oint_\gamma \frac{\Pi(s')}{s'-s} ds'$$

Deform integration path:

$$\Pi(s) - \Pi(0) = \frac{s}{\pi} \int_{4M_\pi^2}^{\infty} \frac{\mathrm{Im}\Pi(s')}{(s'-s-i\epsilon)s'} ds'$$

HVP contribution to $(g-2)_\mu$

$$a_\mu^{\mathrm{HVP}} = \frac{m_\mu^2}{12\pi^3} \int_{s_{\mathrm{thr}}}^{\infty} ds\, \frac{\hat{K}(s)}{s}\, \sigma(e^+e^- \to \mathrm{hadrons})$$

- basic principles: unitarity and analyticity
- direct relation to experiment: total hadronic cross section $\sigma(e^+e^- \to \mathrm{hadrons})$
- can be systematically improved: dedicated e^+e^- program (BaBar, Belle, BESIII, CMD3, KLOE2, SND)

Hadronic light-by-light (HLbL) scattering

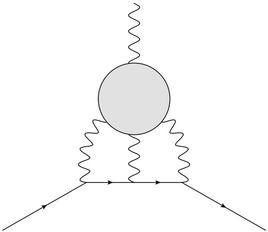

- previously only model calculations
- uncertainty estimate based rather on consensus than on a systematic method
- with recent progress on HVP, HLbL starts to dominate the theory uncertainty
- progress with lattice QCD and dispersive approach

Two-pion contribution to HVP

- $\pi\pi$ contribution amounts to more than 70% of HVP contribution
- responsible for a similar fraction of HVP uncertainty
- unitarity relation for $\pi\pi$ contribution to HVP: pion vector form factor (VFF)

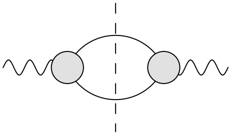

$$: \quad \sigma(e^+e^- \to \pi^+\pi^-) \propto |F_\pi^V(s)|^2$$

Two-pion contribution to HVP

- VFF itself fulfils again a unitarity relation:

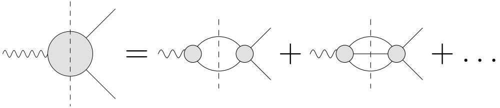

- use the constraints of analyticity and unitarity to better understand uncertainties in HVP $\pi\pi$ channel

  $\rightarrow$ de Trocóniz, Ynduráin, 2001, 2004; Leutwyler, Colangelo 2002, 2003; Ananthanarayan et al. 2013, 2016

Dispersive representation of pion VFF

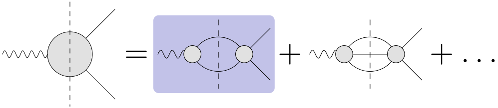

$$F_\pi^V(s) = \Omega_1^1(s) \times G_\omega(s) \times G_{\text{in}}^N(s)$$

- Omnès function with elastic $\pi\pi$-scattering P-wave phase shift $\delta_1^1(s)$ as input:

$$\Omega_1^1(s) = \exp\left\{ \frac{s}{\pi} \int_{4M_\pi^2}^{\infty} ds' \frac{\delta_1^1(s')}{s'(s'-s)} \right\}$$

Dispersive representation of pion VFF

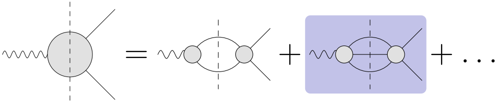

$$F_\pi^V(s) = \Omega_1^1(s) \times \boxed{G_\omega(s)} \times G_{\text{in}}^N(s)$$

- isospin-breaking 3π intermediate state: negligible apart from ω resonance (ρ–ω interference effect)

$$G_\omega(s) = 1 + \frac{s}{\pi}\int_{9M_\pi^2}^\infty ds' \frac{\mathrm{Im} g_\omega(s')}{s'(s'-s)} \left(\frac{1-\frac{9M_\pi^2}{s'}}{1-\frac{9M_\pi^2}{M_\omega^2}}\right)^4 ,$$

$$g_\omega(s) = 1 + \epsilon_\omega \frac{s}{(M_\omega - \frac{i}{2}\Gamma_\omega)^2 - s}$$

Dispersive representation of pion VFF

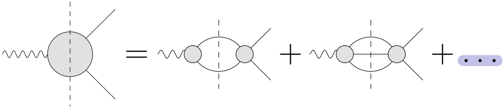

$$F_\pi^V(s) = \Omega_1^1(s) \times G_\omega(s) \times \boxed{G_{\rm in}^N(s)}$$

- heavier intermediate states: 4π (mainly $\pi^0\omega$), $\bar{K}K, \ldots$
- described in terms of a conformal polynomial with cut starting at $\pi^0\omega$ threshold

$$G_{\rm in}^N(s) = 1 + \sum_{k=1}^{N} c_k \left(z^k(s) - z^k(0)\right)$$

- correct P-wave threshold behaviour imposed

Input and systematic uncertainties

- elastic $\pi\pi$-scattering P-wave phase shift $\delta_1^1(s)$ from Roy-equation analysis, including uncertainties

  $\rightarrow$ Ananthanarayan et al., 2001; Caprini et al., 2012

- high-energy continuation of phase shift above validity of Roy equations
- ω width
- systematics in conformal polynomial: order N, one mapping parameter

Free fit parameters

- value of the elastic $\pi\pi$-scattering P-wave phase shift δ_1^1 at two points (0.8 GeV and 1.15 GeV)
- ρ–ω mixing parameter ϵ_ω
- ω mass
- energy rescaling for the experimental input, which allows for a calibration uncertainty
- $N-1$ coefficients in the conformal polynomial

VFF fit to the following data

- time-like cross section data from high-statistics e^+e^- experiments SND, CMD-2, BaBar, KLOE
- space-like VFF data from NA7
- Eidelman–Łukaszuk bound on inelastic phase:

  $\rightarrow$ Eidelman, Łukaszuk, 2004
- iterative fit routine including full experimental covariance matrices and avoiding D'Agostini bias

  $\rightarrow$ D'Agostini, 1994; Ball et al. (NNPDF) 2010

VFF fit results

	χ^2/dof	M_ω [MeV]	$10^3 \times \xi_j$	$\delta_1^1(s_0)$ [°]	$\delta_1^1(s_1)$ [°]	$10^3 \times \epsilon_\omega$
SND	$51.9/37 = 1.40$	$781.49(32)(2)$	$0.0(6)(0)$	$110.5(5)(8)$	$165.7(0.3)(2.4)$	$2.03(5)(2)$
CMD-2	$87.4/74 = 1.18$	$781.98(29)(1)$	$0.0(6)(0)$	$110.5(5)(8)$	$166.4(0.4)(2.4)$	$1.88(6)(2)$
BaBar	$299.1/262 = 1.14$	$781.86(14)(1)$	$0.0(2)(0)$	$110.4(3)(7)$	$165.7(0.2)(2.5)$	$2.04(3)(2)$
KLOE″	$222.5/185 = 1.20$	$781.81(16)(3)$	$\begin{cases} 0.5(2)(0) \\ -0.3(2)(0) \\ -0.2(3)(0) \end{cases}$	$110.3(2)(6)$	$165.6(0.1)(2.4)$	$1.98(4)(1)$
Energy scan	$152.5/119 = 1.28$	$781.75(22)(1)$		$110.4(3)(8)$	$166.0(0.2)(2.4)$	$1.97(4)(2)$
All e^+e^-	$731.6/582 = 1.26$	$781.68(9)(4)$		$110.4(1)(7)$	$165.8(0.1)(2.4)$	$2.02(2)(3)$
All e^+e^-, NA7	$776.2/627 = 1.24$	$781.68(9)(3)$		$110.4(1)(7)$	$165.7(0.1)(2.4)$	$2.02(2)(3)$

- 1$^{\text{st}}$ error: fit uncertainty; 2$^{\text{nd}}$ error: systematics
- fit uncertainty inflated by $\sqrt{\chi^2/\mathrm{dof}}$

VFF fit results

- good fits to all experiments possible (p-value around 3% to 14%) with a few caveats:
  - either M_ω or energy recalibration has to be fit (practically identical results)
  - two outliers in KLOE08 set (> 30 units in χ^2)
  - BESIII covariance matrix cannot be used
- well-known discrepancy between BaBar and KLOE $\Rightarrow$ fit all data sets and inflate errors by $\sqrt{\chi^2/\mathrm{dof}}$
- inelastic effects dominate uncertainty for $(g-2)_\mu$

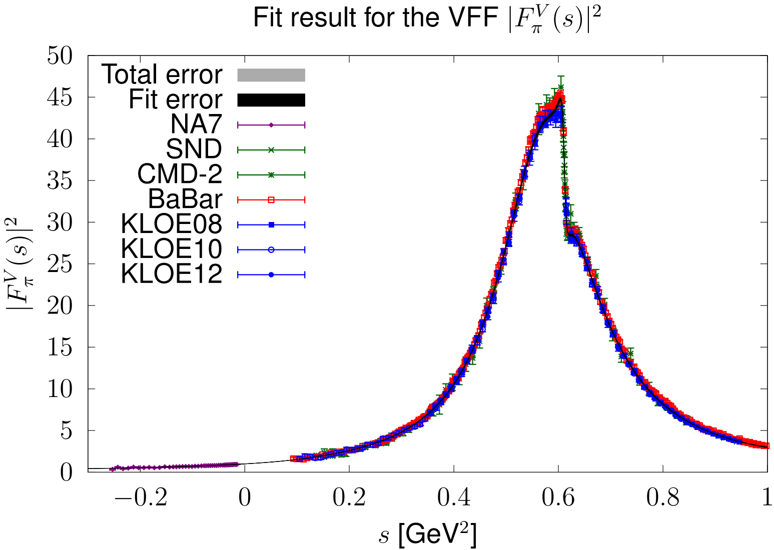
Fit result for the VFF $|F_\pi^V(s)|^2$
Total error
Fit error
NA7
SND
CMD-2
BaBar
KLOE08
KLOE10
KLOE12
$|F_\pi^V(s)|^2$
s [GeV^2]
50
45
40
35
30
25
20
15
10
5
0
−0.2
0
0.2
0.4
0.6
0.8
1

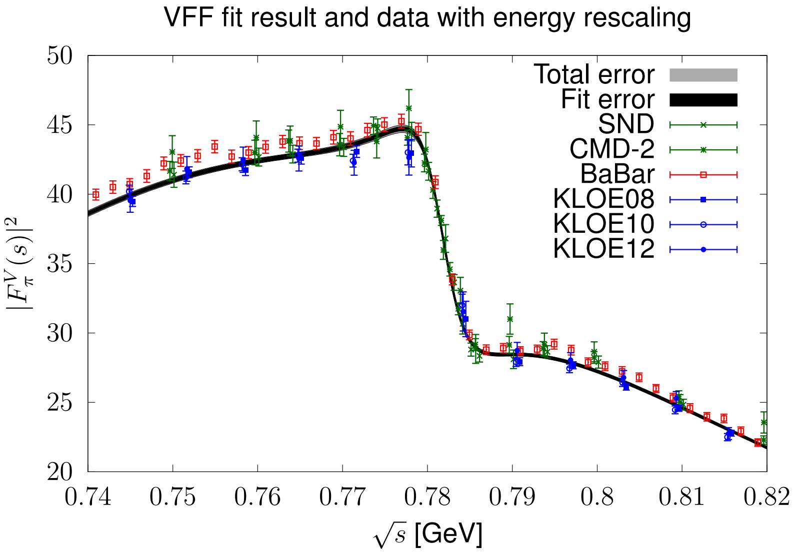
VFF fit result and data with energy rescaling
Total error
Fit error
SND
CMD-2
BaBar
KLOE08
KLOE10
KLOE12
$|F_\pi^V(s)|^2$
$\sqrt{s}$ [GeV]
50
45
40
35
30
25
20
0.74
0.75
0.76
0.77
0.78
0.79
0.8
0.81
0.82

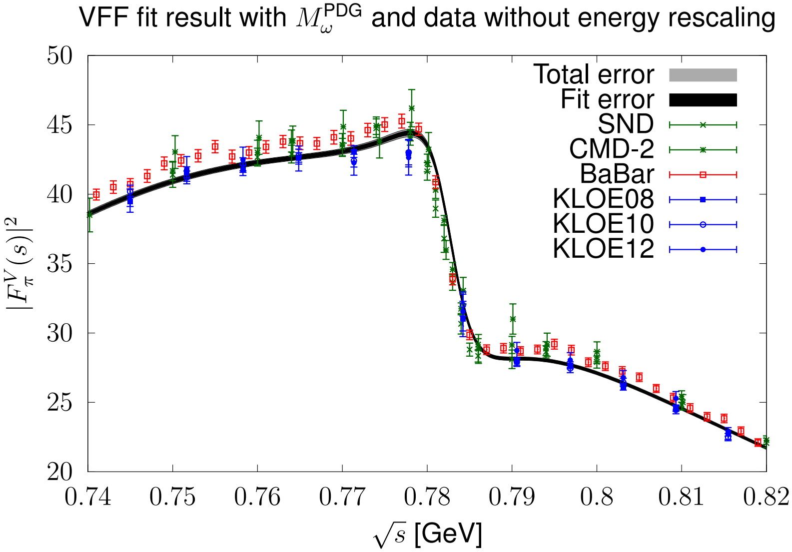
VFF fit result with M_ω^{PDG} and data without energy rescaling
Total error
Fit error
SND
CMD-2
BaBar
KLOE08
KLOE10
KLOE12
$|F_\pi^V(s)|^2$
50
45
40
35
30
25
20
0.74
0.75
0.76
0.77
0.78
0.79
0.8
0.81
0.82
$\sqrt{s}$ [GeV]

Fit result for the VFF $|F_\pi^V(s)|^2$

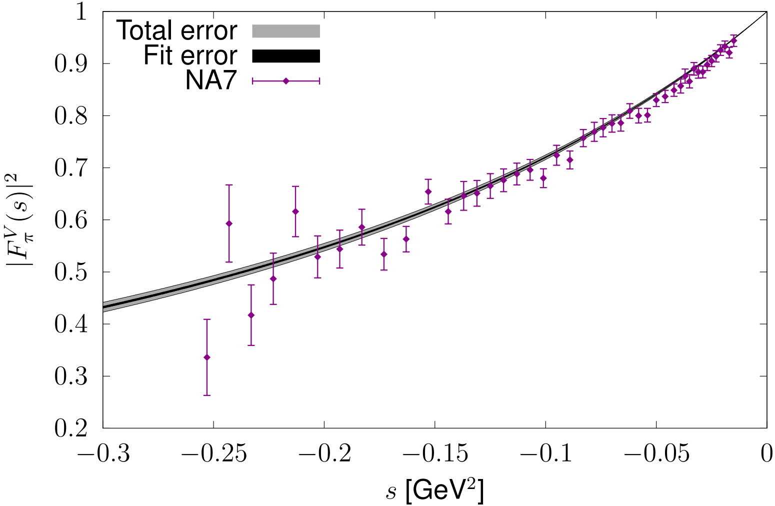

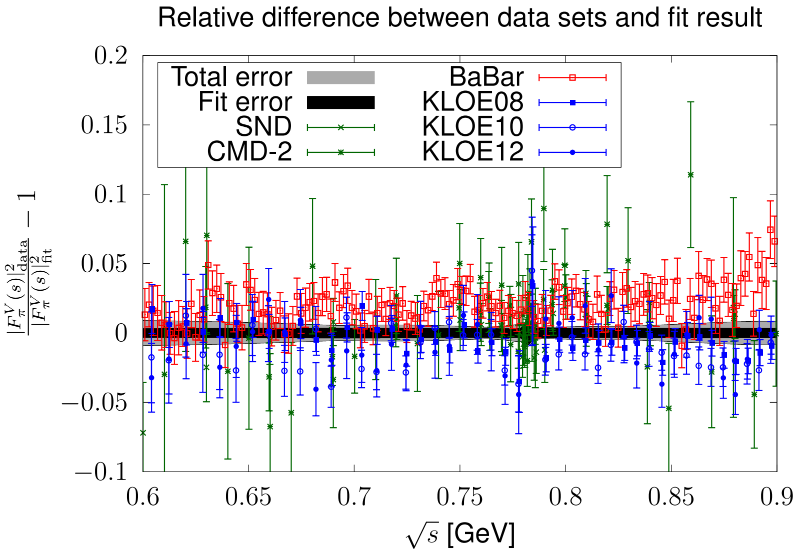
Relative difference between data sets and fit result
Total error
Fit error
SND
CMD-2
BaBar
KLOE08
KLOE10
KLOE12
$\frac{|F_\pi^V(s)|^2_{\text{data}}}{|F_\pi^V(s)|^2_{\text{fit}}} - 1$
0.2
0.15
0.1
0.05
0
−0.05
−0.1
0.6
0.65
0.7
0.75
0.8
0.85
0.9
$\sqrt{s}$ [GeV]

Contribution to $(g-2)_\mu$

- low-energy $\pi\pi$ contribution:

$$a_\mu^{\mathrm{HVP},\pi\pi}|_{\leq 0.63\,\text{GeV}} = 132.8(0.4)(1.0) \times 10^{-10}$$

$\Rightarrow$ compare to $131.1(1.0) \rightarrow$ KNT18, $132.9(8) \rightarrow$ Ananthanarayan et al., 2018

- $\pi\pi$ contribution up to 1 GeV:

$$a_\mu^{\mathrm{HVP},\pi\pi}|_{\leq 1\,\text{GeV}} = 495.0(1.5)(2.1) \times 10^{-10}$$

Result for $a_\mu^{\mathrm{HVP},\pi\pi}$ below 1 GeV

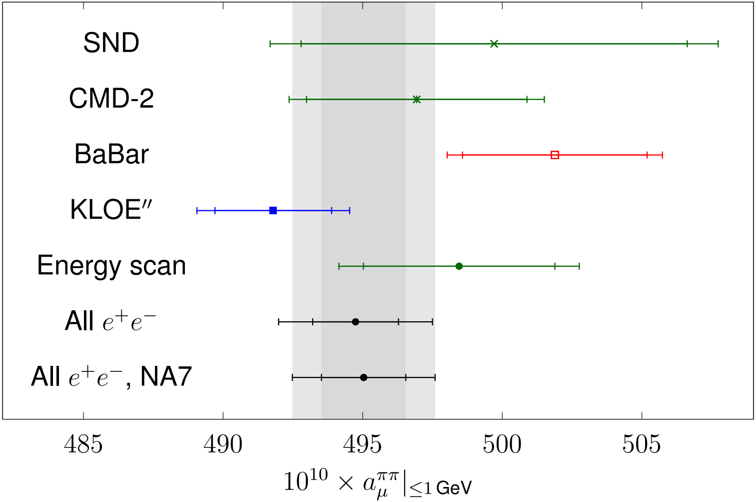

Improved determination of $\delta_1^1(s)$

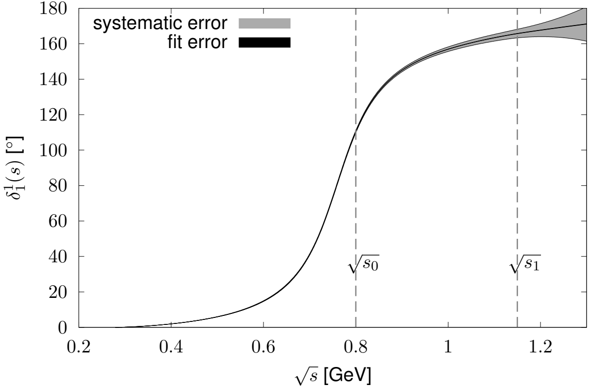

$$\delta_1^1(s_0) = 110.4(1)(7)^\circ = 110.4(7)^\circ$$

$$\delta_1^1(s_1) = 165.7(0.1)(2.4)^\circ = 165.7(2.4)^\circ$$

Determination of the pion charge radius

$$F_\pi^V(s) = 1 + \frac{1}{6}\langle r_\pi^2\rangle s + \mathcal{O}(s^2)$$

DR for F_π^V implies sum rule for charge radius:

$$\langle r_\pi^2\rangle = \frac{6}{\pi}\int_{4M_\pi^2}^\infty ds \frac{\mathrm{Im} F_\pi^V(s)}{s^2} = 0.429(4)\,\text{fm}^2$$

together with $\langle r_\pi^2\rangle = 0.432(4) \rightarrow$ Ananthanarayan et al., 2017

triggered a revision of the PDG value:

PDG 2018: $\langle r_\pi^2\rangle = 0.452(11)\,\text{fm}^2$

PDG 2019: $\langle r_\pi^2\rangle = 0.434(5)\,\text{fm}^2$

(model-dependent $eN \rightarrow e\pi N$ now excluded)

Dispersive approach

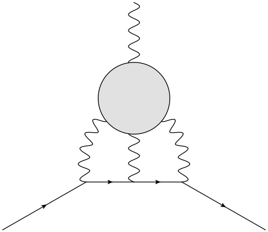

- make use of fundamental principles:
  - gauge invariance, crossing symmetry
  - unitarity, analyticity
- relate HLbL to experimentally accessible quantities

BTT Lorentz decomposition

Lorentz decomposition of the HLbL tensor:

$\to$ Bardeen, Tung (1968) and Tarrach (1975)

$$\Pi^{\mu\nu\lambda\sigma}(q_1, q_2, q_3) = \sum_i T_i^{\mu\nu\lambda\sigma} \Pi_i(s, t, u; q_j^2)$$

- Lorentz structures manifestly gauge invariant
- scalar functions Π_i free of kinematic singularities
  $\Rightarrow$ dispersion relation in the Mandelstam variables

Dispersive representation

- write down a double-spectral (Mandelstam) representation for the HLbL tensor
- split the HLbL tensor according to the sum over intermediate (on-shell) states in unitarity relations

$$\Pi_{\mu\nu\lambda\sigma} = \Pi^{\pi^0\text{-pole}}_{\mu\nu\lambda\sigma} + \Pi^{\text{box}}_{\mu\nu\lambda\sigma} + \Pi^{\pi\pi}_{\mu\nu\lambda\sigma} + \dots$$

Dispersive representation

- write down a double-spectral (Mandelstam) representation for the HLbL tensor
- split the HLbL tensor according to the sum over intermediate (on-shell) states in unitarity relations

$$\Pi_{\mu\nu\lambda\sigma} = \boxed{\Pi^{\pi^0\text{-pole}}_{\mu\nu\lambda\sigma}} + \Pi^{\text{box}}_{\mu\nu\lambda\sigma} + \Pi^{\pi\pi}_{\mu\nu\lambda\sigma} + \dots$$

one-pion intermediate state

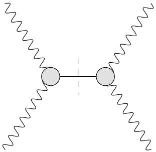

Dispersive representation

- write down a double-spectral (Mandelstam) representation for the HLbL tensor
- split the HLbL tensor according to the sum over intermediate (on-shell) states in unitarity relations

$$\Pi_{\mu\nu\lambda\sigma} = \Pi^{\pi^0\text{-pole}}_{\mu\nu\lambda\sigma} + \boxed{\Pi^{\text{box}}_{\mu\nu\lambda\sigma}} + \Pi^{\pi\pi}_{\mu\nu\lambda\sigma} + \dots$$

two-pion intermediate state in both channels

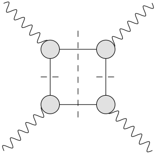

Dispersive representation

- write down a double-spectral (Mandelstam) representation for the HLbL tensor
- split the HLbL tensor according to the sum over intermediate (on-shell) states in unitarity relations

$$\Pi_{\mu\nu\lambda\sigma} = \Pi^{\pi^0\text{-pole}}_{\mu\nu\lambda\sigma} + \Pi^{\text{box}}_{\mu\nu\lambda\sigma} + \boxed{\Pi^{\pi\pi}_{\mu\nu\lambda\sigma}} + \dots$$

two-pion intermediate state in first channel

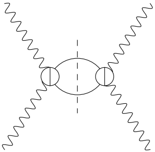

Dispersive representation

- write down a double-spectral (Mandelstam) representation for the HLbL tensor
- split the HLbL tensor according to the sum over intermediate (on-shell) states in unitarity relations

$$\Pi_{\mu\nu\lambda\sigma} = \Pi^{\pi^0\text{-pole}}_{\mu\nu\lambda\sigma} + \Pi^{\text{box}}_{\mu\nu\lambda\sigma} + \Pi^{\pi\pi}_{\mu\nu\lambda\sigma} + \dots$$

higher intermediate states

Pion pole

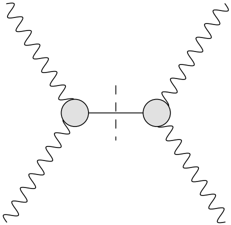

$$\bar{\Pi}_1^{\pi^0\text{-pole}} = \frac{\mathcal{F}_{\pi^0\gamma^*\gamma^*}(q_1^2, q_2^2)\mathcal{F}_{\pi^0\gamma^*\gamma}(q_3^2, 0)}{q_3^2 - M_\pi^2}$$

$\bar{\Pi}_2^{\pi^0\text{-pole}}$ via crossing symmetry

- input: doubly-virtual and singly-virtual pion transition form factors $\mathcal{F}_{\gamma^*\gamma^*\pi^0}$ and $\mathcal{F}_{\gamma^*\gamma\pi^0}$
- dispersive analysis of transition form factor:
  $a_\mu^{\pi^0\text{-pole}} = 62.6^{+3.0}_{-2.5} \times 10^{-11}$

  → Hoferichter et al., PRL 121 (2018) 112002, JHEP 10 (2018) 141

Box contribution

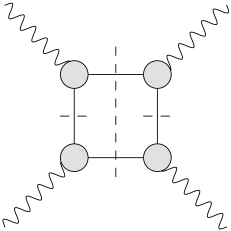

- simultaneous two-pion cuts in two channels
- Mandelstam representation explicitly constructed
- q^2-dependence: pion VFF $F_\pi^V(q_i^2)$ for each off-shell photon factor out
- Wick rotation: integrate over space-like momenta
- dominated by low energies $\leq$ 1 GeV
- result: $a_\mu^{\pi\text{-box}} = -15.9(2) \times 10^{-11}$

Fit result for the VFF $|F_\pi^V(s)|^2$

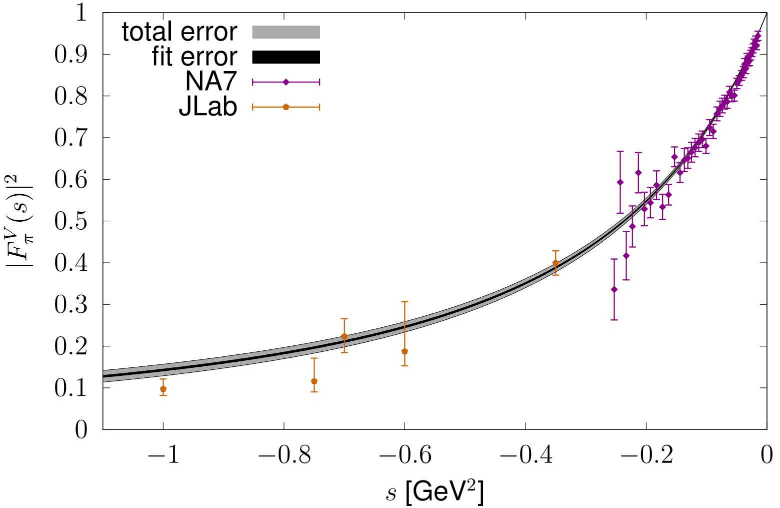

(the JLab data are not used in the fit)

Rescattering contribution

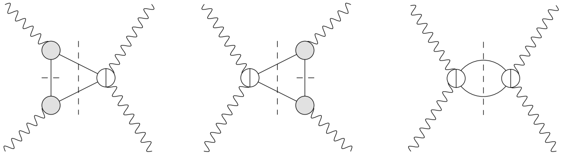

- neglect left-hand cut due to multi-particle intermediate states in crossed channel
- two-pion cut in only one channel:

$$\Pi_i^{\pi\pi} = \frac{1}{2}\bigg(\frac{1}{\pi}\int_{4M_\pi^2}^{\infty} dt' \frac{\mathrm{Im}\Pi_i^{\pi\pi}(s,t',u')}{t'-t} + \frac{1}{\pi}\int_{4M_\pi^2}^{\infty} du' \frac{\mathrm{Im}\Pi_i^{\pi\pi}(s,t',u')}{u'-u}$$
$$+ \text{fixed-}t$$
$$+ \text{fixed-}u\bigg)$$

Rescattering contribution

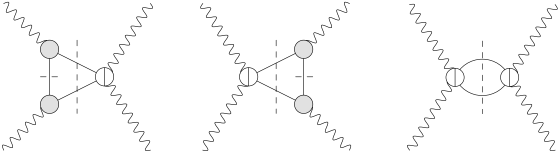

- expansion into partial waves
- unitarity gives imaginary parts in terms of helicity amplitudes for $\gamma^*\gamma^{(*)} \to \pi\pi$:

$$\mathrm{Im}_{\pi\pi} h^J_{\lambda_1\lambda_2,\lambda_3\lambda_4}(s) \propto \sigma_\pi(s) h_{J,\lambda_1\lambda_2}(s) h^*_{J,\lambda_3\lambda_4}(s)$$

- framework valid for arbitrary partial waves
- resummation of PW expansion reproduces full result: checked for pion box

The subprocess

Omnès solution of unitarity relation for $\gamma^*\gamma^* \to \pi\pi$ helicity partial waves:

$$h_i(s) = \Delta_i(s) + \frac{\Omega(s)}{\pi} \int_{4M_\pi^2}^{\infty} ds' \frac{K_{ij}(s,s') \sin\delta(s') \Delta_j(s')}{|\Omega(s')|}$$

- $\Delta_i(s)$: inhomogeneity due to left-hand cut
- $\Omega(s)$: Omnès function, input is $\pi\pi$ phase shift $\delta(s)$
- $K_{ij}(s,s')$: integration kernels
- S-waves: kernels emerge from a 2×2 system for $h_{0,++}$ and $h_{0,00}$ and two scalar functions $A_{1,2}$

Topologies in the rescattering contribution

Our S-wave solution for $\gamma^*\gamma^* \to \pi\pi$:

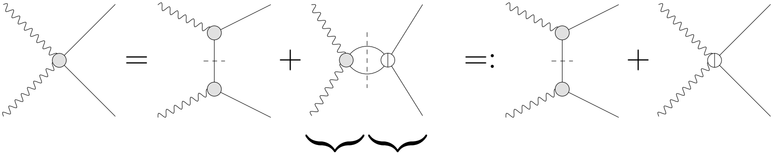

recursive PWE, no LHC

Two-pion contributions to HLbL:

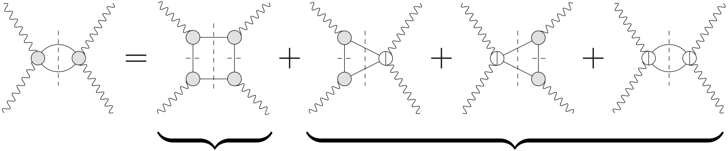

pion box rescattering contribution

S-wave rescattering contribution

- pion-pole approximation to left-hand cut
  $\Rightarrow q^2$-dependence given by F_π^V
- phase shifts based on modified inverse-amplitude method ($f_0(500)$ parameters accurately reproduced)
- result for S-waves:

$$a_{\mu,J=0}^{\pi\pi,\pi\text{-pole LHC}} = -8(1) \times 10^{-11}$$

Extension to D-waves

- D-waves describe $f_2(1270)$ resonance in terms of $\pi\pi$ rescattering
- inclusion of higher left-hand cuts (ρ, ω resonances) necessary to reproduce observed $f_2(1270)$ resonance peak in on-shell $\gamma\gamma \to \pi\pi$
- NWA for vector resonance LHC with $V\pi\gamma$ interaction

$$\mathcal{L} = eC_V \epsilon^{\mu\nu\lambda\sigma} F_{\mu\nu} \partial_\lambda \pi V_\sigma$$

- coupling C_V related to decay width $\Gamma(V \to \pi\gamma)$
- off-shell behaviour described by resonance transition form factors $F_{V\pi}(q^2)$

Topologies in the D-wave Omnès solution

Omnès solution for $\gamma^*\gamma^* \to \pi\pi$ with higher left-hand cuts provides the following:

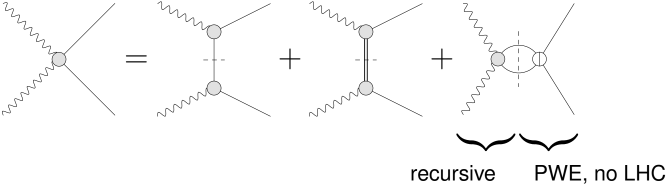

D-wave solution

- modified Omnès representation

  $\rightarrow$ García-Martín, Moussallam, 2010

- sum rules for unsubtracted DR are nearly fulfilled (corrections due to higher intermediate states)
- complete solution of the off-shell 5×5 D-wave Roy–Steiner system
- large space-like q_i^2: anomalous thresholds in resonance PW appear $\Rightarrow$ solution in terms of a path deformation
- numerics for contribution to a_μ in progress

HVP

- precise dispersive determination of pion VFF
- comprehensive analysis of uncertainties in $\pi\pi$ channel
- valuable to corroborate uncertainties of direct integration methods
- precise prediction for low-energy region, but useful up to 1 GeV:

$$a_\mu^{\mathrm{HVP},\pi\pi}|_{\leq 1\,\mathrm{GeV}} = 495.0(1.5)(2.1) \times 10^{-10}$$

- side-products: improved determination of $\pi\pi$ P-wave phase shift; pion charge radius

HLbL

- very precise evaluation of HLbL pion-box contribution:

$$a_\mu^{\pi\text{-box}} = -15.9(2) \times 10^{-11}$$

- precise prediction for S-wave $\pi\pi$-rescattering contribution with pion-pole left-hand cut:

$$a_{\mu,J=0}^{\pi\pi,\pi\text{-pole LHC}} = -8(1) \times 10^{-11}$$

- D-wave numerics work in progress
- contributions beyond $\pi\pi$ and matching to pQCD/OPE constraints work in progress $\rightarrow$ Bijnens et al., 2019

Summary

- our dispersive approach to HVP and HLbL is based on fundamental principles:
  - gauge invariance, crossing symmetry (for HLbL)
  - unitarity, analyticity
- we are focusing on the lightest intermediate states
- relation to experimentally accessible (or again with data dispersively reconstructed) quantities
- precise numerical evaluation of two-pion contributions
- a step towards a model-independent calculation of a_μ

Backup

SM contributions to $(g-2)_\mu$

	$10^{11} \times a_\mu$	$10^{11} \times \Delta a_\mu$	
BNL E821	$116\,592\,089$	63	→ PDG 2016
QED total	$116\,584\,718.97$	0.07	→ Aoyama et al. 2012, 2017
EW	153.6	1.0	→ Gnendiger et al. 2013
LO HVP	$6\,932.7$	24.6	→ Keshavarzi et al. 2018
NLO HVP	-98.2	0.4	→ Keshavarzi et al. 2018
NNLO HVP	12.4	0.1	→ Kurz et al. 2014
LO HLbL	102	39	→ Nyffeler 2017
NLO HLbL	3	2	→ Colangelo et al. 2014
Hadronic total	6952	46	
Theory total	$116\,591\,825$	46	

SM contributions to $(g-2)_\mu$

	$10^{11} \times a_\mu$	$10^{11} \times \Delta a_\mu$	
BNL E821	$116\,592\,089$	63	→ PDG 2016
QED total	$116\,584\,718.97$	0.07	→ Aoyama et al. 2012, 2017
EW	153.6	1.0	→ Gnendiger et al. 2013
LO HVP	$6\,931$	34	→ Davier et al. 2017
NLO HVP	-98.2	0.4	→ Keshavarzi et al. 2018
NNLO HVP	12.4	0.1	→ Kurz et al. 2014
LO HLbL	102	39	→ Nyffeler 2017
NLO HLbL	3	2	→ Colangelo et al. 2014
Hadronic total	6950	52	
Theory total	$116\,591\,823$	52	